Acta Cryst E CRYSTALLOGRAPHIC COMMUNICATIONS

ISSN 2056-9890

Crystal structure and Hirshfeld surface analysis of 6-[4-(1-cyclohexyl-1*H*-tetrazol-5-yl)butoxy]-8-nitro-3,4-dihydroquinolin-2(1*H*)-one

Arnab Dutta,[a] Yogesh Dhasmana,[a] T. P. Mohan,[b] B. Selvakumar[b] and Deepak Chopra[a]*

[a]Department of Chemistry, Indian Institute of Science Education and Research Bhopal, Bhauri Bhopal 462066, India, and [b]Bioneeds India Private Limited, P-3, Peenya Industrial Area, 1st Main Road, Peenya 1st stage, Bangalore 560094, Karnataka., India. *Correspondence e-mail: dchopra@iiserb.ac.in

Received 3 February 2025
Accepted 25 February 2025

Edited by B. Therrien, University of Neuchâtel, Switzerland

Keywords: crystal structure; intermolecular interaction; crystal packing; molecular conformation; Hirshfeld surface.

CCDC reference: 2426771

Supporting information: this article has supporting information at journals.iucr.org/e

The crystal structure of 6-[4-(1-cyclohexyl-1*H*-tetrazol-5-yl)butoxy]-8-nitro-3,4-dihydroquinolin-2(1*H*)-one, $C_{20}H_{26}N_6O_4$ (**I**), was characterized by single-crystal X-ray diffraction. The primary focus was to establish the position of the nitro group, the molecular conformation, and the role of intermolecular interactions towards the crystal packing of **I**. The crystalline structure is mainly consolidated by π–π, C—H···O, C—H···N, N···C(π) and O···C(π) interactions. The contributions of different interactions towards the crystal packing were further analyzed using Hirshfeld surface and fingerprint plots.

1. Introduction

Cilostazol is an important active pharmaceutical ingredient used to treat intermittent claudication associated with peripheral vascular disease (Lauters & Wilkin, 2002). However, cilostazol has the potential to generate nitroso impurities. The pharmaceutical industry is subject to stringent regulations to control genotoxic nitrosamine impurities in medications, as these compounds pose significant health risks (Vikram *et al.*, 2024). Therefore, investigating the presence of nitrosamine impurities is crucial.

Given the possibility of nitroso impurity formation, it is essential to identify the specific site on cilostazol where nitrosation may occur. In this study, we attempted to synthesize *N*-nitroso cilostazol using a standard method (Lopez-Rodriguez *et al.*, 2020). Unexpectedly, instead of obtaining the anticipated product – 6-[4-(1-cyclohexyl-1*H*-tetrazol-5-yl) butoxy]-1-nitroso-3,4-dihydroquinolin-2(1*H*)-one (*N*-nitroso cilostazol) – we isolated a different compound, referred to as **I**. This compound was fully characterized using ^{1}H NMR and LC-MS, spectroscopy and single-crystal X-ray diffraction.

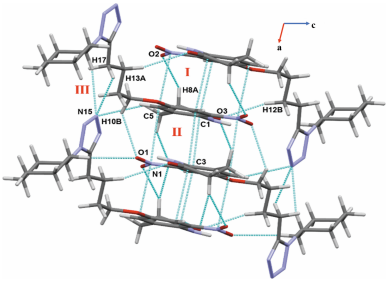

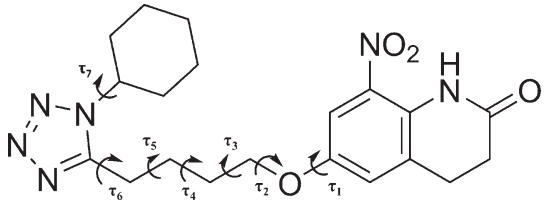

2. Structural commentary

The molecular structure features a dihydroquinolinone moiety (N2/C1–C9/O3) and a tetrazole moiety composed of two fused six-membered rings (C1–C6, **B**, and C1/C6–C9/N2, **A**) and a

OPEN ACCESS
Published under a CC BY 4.0 licence

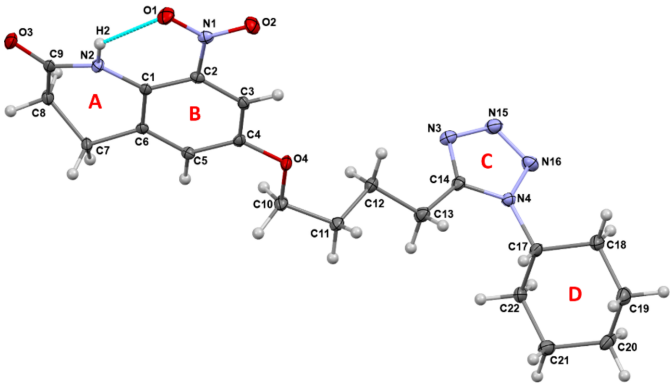

Figure 1
The molecular structure of **I** with 50% probability level ellipsoids. The dotted line indicates the intramolecular N2—H2···O1 interaction.

five-membered ring (C14/N3/N15/N16/N4, *C*), respectively (Fig. 1). The dihedral angle between the plane through ring **B** and atoms O4, C10, C11 and the mean plane through ring **C** and atoms C13, C12, C11 is 82.46 (6)°. The butoxy chain exhibits rotational freedom, contributing to the conformational flexibility of the molecule. The various torsions of the butoxy chain are represented by τ_2, τ_3, τ_4, τ_5, and τ_6, and listed in Table 1. The C2 and C4 carbon atoms are connected to the nitro and alkoxy substituents, respectively, and the presence of two sp^3-hybridized carbon atoms (C7 and C8) makes ring **A** non-planar. The puckering parameters (Cremer & Pople, 1975) generated by *PLATON* (Spek, 2020) were obtained for the different rings. For ring **A**, the puckering parameters are Q = 0.420 (2) Å, θ = 65.9 (3)° and φ = 25.1 (3)°, the value of θ indicating a screw-boat conformation (Boeyens, 1978). Atom N4 of ring **C** is linked to the cyclohexyl ring (C17–C22, *D*) [Q = 0.582 (3) Å, θ = 1.1 (3)° and φ = 138 (11)°]. The value of θ is very close to zero, thus indicating a chair conformation for ring **D**. The most acidic hydrogen atom (H2) is involved in the formation of an intramolecular hydrogen bond with the O1 atom of the nitro group [N2···O1 = 2.650 (3) Å, ∠N—H···O = 128°].

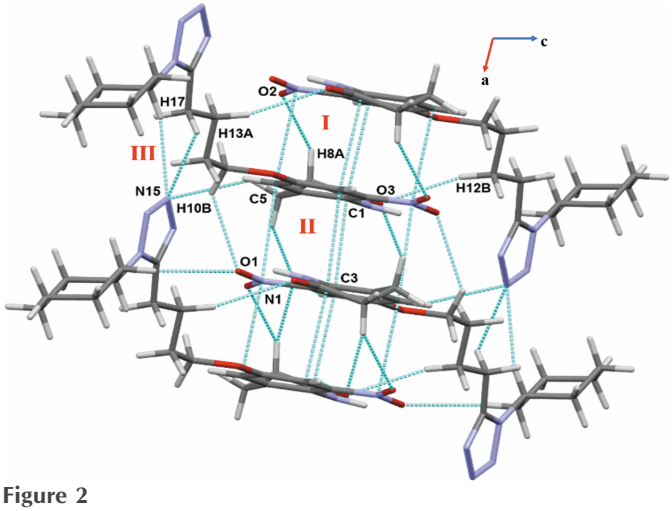

Figure 2
Crystal packing extending along the *a*-axis *via* π–π stacking, N(π-hole)···C(π), C—H···O and C—H···N interactions.

Table 1
Torsion angles (°) of the butoxy chain in **I**, **IA**, **IC** (see *Database survey*).

Torsion angle	**I**	**IA**	**IC**
τ_1	177.7 (2)	−7.9 (2)	4.1 (2)
τ_2	−179.4 (2)	174.6 (1)	175.8 (1)
τ_3	−74.1 (2)	174.8 (1)	−174.7 (1)
τ_4	−171.1 (2)	70.9 (1)	178.5 (1)
τ_5	176.1 (2)	179.6 (1)	−64.6 (2)
τ_6	168.9 (2)	−111.7 (1)	−94.9 (2)

Table 2
Intermolecular interactions (Å, °) present in **I**.

Motif	*D*—*X*···*Y*	*D*—*X*	*X*···*Y*	*D*···*Y*	∠*D*—*X*···*Y*
I[vi]	C8—H8*A*···O2—N1	0.99	2.71	3.467 (2)	133
	C3(π)···C1(π)	–	3.261 (3)	–	–
	N1···C5(π)	–	3.230 (3)	–	–
	C12—H12*B*···O3—C9	0.99	2.62	3.553 (3)	157
II[iii]	C10—H10*B*···O1—N1	0.99	2.74	3.526 (3)	136
	C3(π)···C1(π)	–	3.207 (3)	–	–
	N1···C5(π)	–	3.241 (3)	–	–
III[ii]	C17—H17···N15	1.00	2.73	3.705 (3)	165
	C13—H13*A*···N15	0.99	2.80	3.646 (3)	144
IV[vii]	C18—H18*A*···O1—N1	0.99	2.59	3.527 (3)	157
	C14(π)···O2	–	3.146 (3)	–	–
V[i]	C3—H3···O3—C9	0.95	2.75	3.681 (3)	168
	O4···C8—H8*B*	0.99	2.55	3.453 (3)	151
VI[v]	C8—H8*A*···O3—C9	0.99	2.57	3.409 (3)	142
VII[iv]	C7—H7*A*···O3—C9	0.99	2.35	3.170 (2)	140

Symmetry codes: (i) $x, y+1, z$; (ii) $x-1, y, z$; (iii) $-x, -y, -z+1$; (iv) $-x, -1-y, 1-z$; (v) $-x+1, -y-1, -z+1$; (vi) $-x+1, -y, -z+1$; (vii) $-x+1, -y+1, -z+1$.

3. Supramolecular features

The crystal packing was further analysed by *Mercury* (Version 2024.1.0; Macrae *et al.*, 2020). The crystal packing along the *a*-axis shows that the molecules form three motifs by inversion symmetry, I, II and III, respectively (Fig. 2, Table 2). The motifs I and II are consolidated by π–π stacking, N(π-hole)···C(π) and C—H···O hydrogen-bonding interactions, while motif III contains onlyC—H···N hydrogen bonds (involving H17 and N15 and H13*A* with N15). The π–π stacking occurs in a parallel offset fashion between **B** rings in both motifs I and II, the latter one consisting of a very short π–π interaction between C3(π)···C1(π) with a distance of 3.2067 (3) Å. In the MESP map (Fig. 4*a*), the electropositive blue region over N1 (0.0332 a.u.) shows the π hole for the N1···C5 interaction. In motif III, ring *C* forms C—H···N interactions with the butoxy chain and cyclohexyl ring **D**, which propagate along the *a*-axis direction.

Along the *bc* plane (Fig. 3), motif IV forms a centrosymmetric dimer through C—H···O and O···C(π) interactions, while motif V consists of C3—H3···O3 and C8—H8*B*···O4 interactions. Motif V utilizes translation symmetry along the *b*-axis direction for the packing of molecules in the crystal. The remaining motifs VI and VII are also involved in the formation of C—H···O hydrogen bonds, the latter one shows a significant short contact [C7···O3 = 3.170 (2) Å]. It is noteworthy that atoms H3 and H17, which are attached to hybridized sp^2 carbons, form the most directional C—H···O and C—H···N hydrogen bonds in the crystal packing.

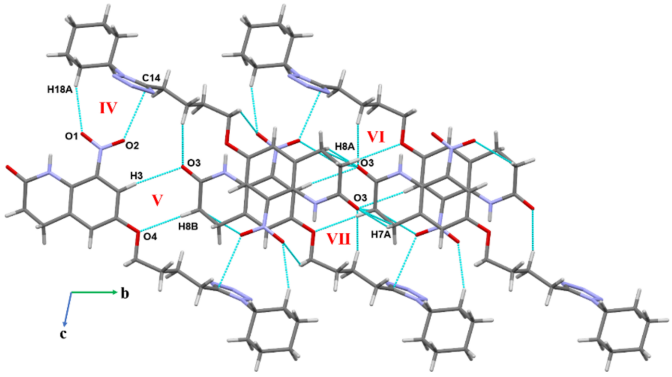

Figure 3
Crystal packing of **I** along the *bc* plane showing C—H···O and O···C(π) interactions.

4. Hirshfeld surface analysis and fingerprint plots

Hirshfeld surface analysis was performed to investigate and visualize the intermolecular interactions present between molecules and most importantly to quantify the individual contributions of different interactions involved in the crystal packing (Spackman *et al.*, 2021). The Hirshfeld surface and the 2D fingerprint plots (Spackman & McKinnon, 2002) were generated using *CrystalExplorer* (version: 21.5) over electrostatic potential range −0.02 a.u. to +0.02 a.u., as depicted in Figs. 4 and 5, respectively. The red spots on the Hirshfeld surface (plotted over d_{norm}) (Fig. 4*b*,*c*,*d*) indicate the presence of intermolecular π–π stacking, C—H···N, C—H···O, O···C(π) and N···C(π) short contacts. In the crystal packing, the relative contributions of the interactions are: O···H/H···O (22.2%), N···H/H···N (17.1%), C(π)···C(π) (3.7%), O···C(π)/C(π)···O (2.6%) and N···C(π)/C(π)···N (2.3%).

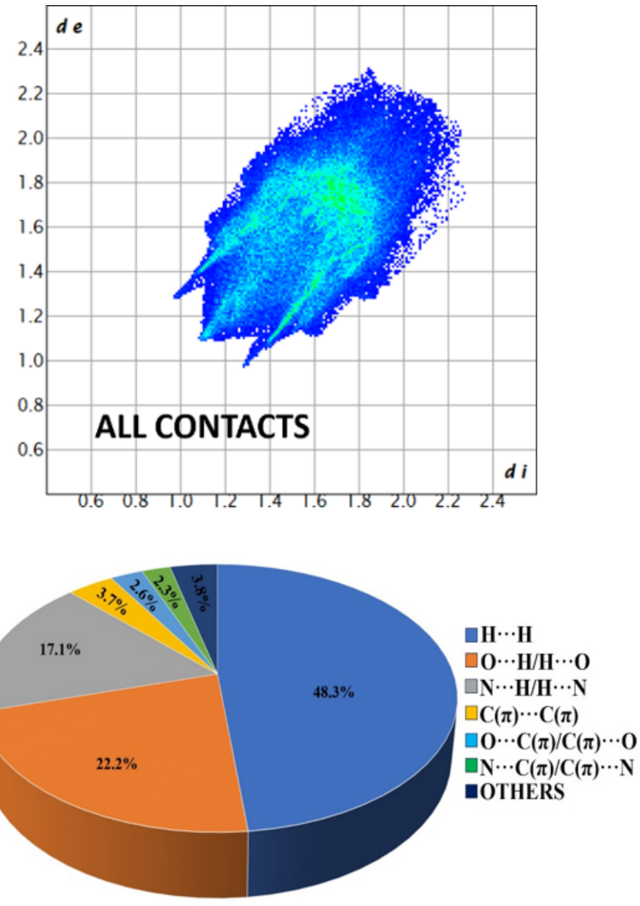

Figure 5
The fingerprint plot showing the overall contribution of all contacts and a diagram showing the percentage of individual contributions in the crystal packing.

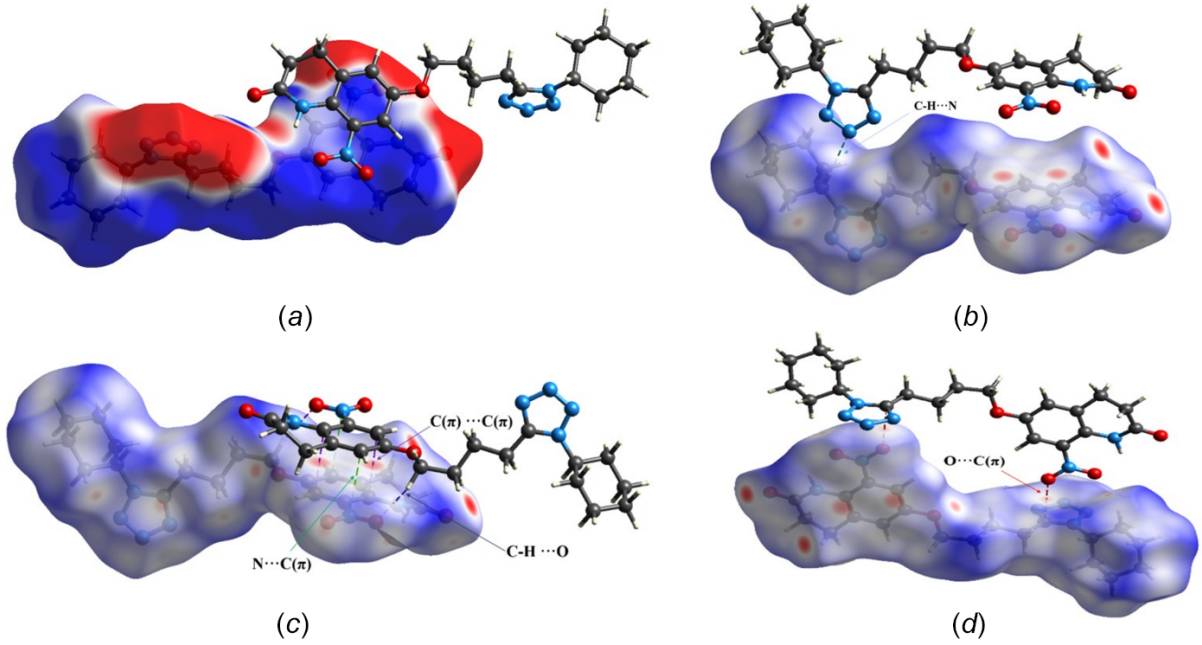

Figure 4
The molecular electrostatic potential map (*a*) and Hirshfeld surface mapped over d_{norm} (*b*, *c*, *d*). Non-covalent interactions are indicated by dashed lines.

5. Database survey

A CSD (Groom *et al.*, 2016) survey for the cilostazol molecule was performed using CCDC ConQuest (version 2024.1.0). The five resulting hits with refcodes OCIKIX, OCIKOD, OCIKUJ (Yoshimura *et al.*, 2017) and XOSGUH, XOSGUH01 (Whittall *et al.*, 2002) report co-crystals of cilostazol and the structures of polymorphic forms of cilostazol.

OCIKIX, OCIKOD and OCIKUJ (Yoshimura *et al.*, 2017) are three co-crystals of cilostazol. Cilostazol is a poorly soluble compound, and in order to increase the solubility, co-crystals of cilostazol with 4-hydroxybenzoic acid, 2,4-dihydroxybenzoic acid and 2,5-dihydroxybenzoic acid (1:1 stoichiometric ratio) have been prepared for different pharmaceutical applications.

XOSGUH and XOSGUH01 (Whittall *et al.*, 2002) feature two unique conformational polymorphic forms of cilostazol. The study shows how the conformational differences can possibly influence the intermolecular forces and packing of the molecules during crystallization. As a result of the conformational flexibility of the butoxy chain, cilostazol crystallizes in two different space groups, $P2_1/n$ (**IC**) and *Pbca* (**IA**). It is observed that **I** exists in two different conformations for the two reported polymorphs of cilostazol. Conformational variations were analysed by generating a molecular overlay diagram, keeping the tetrazole rings fixed for the three molecules (Fig. 6). It is found that **I** and **IC** have similar conformations but differ significantly from **IA**. The magnitudes of the torsion angles (Table 1) indicate that the most significant conformational differences are observed in the butoxy chains.

6. Synthesis and crystallization

Cilostazol (1.00 g, 2.7 mmol) was stirred in 5 mL of dichloroethane for 15 min. Isoamyl nitrite (0.32 g, 2.7 mmol) was added at 273–278 K. The reaction mixture was slowly brought to 298 K and allowed to stir for 1h. The reaction mixture was diluted with water and extracted with dichloromethane twice (2 × 50 mL) and concentrated to dryness to afford 1 g of crude product. The crude product was purified by flash chromatography using 2% methanol:dichloromethane eluent system to afford the title compound (0.35 g, 33%). ^{1}H NMR (400 MHz, dimethyl sulfoxide): δ 9.70 (*s*, 1H), 7.47–7.48 (*d*, J = 2.8 Hz, 1H), 7.36 (*d*, J = 2.8 Hz, 1H), 4.41–4.42 (*m*, 1H), 4.08–4.11 (*m*, 2H), 2.97–3.04 (*m*, 4H), 2.51–2.58 (*m*, 2H), 1.67–1.98 (*m*, 11H), 1.42-1.46 (*m*, 2H), 1.24–1.28 (*m*, 1H), LC/MS (ESI) *m*/*e* 415.2 $[M + H]^+$ calculated for $C_{20}H_{27}N_6O_4$. The crude product was dissolved in isooctane-chloroform (1:1 mixture) and kept at low temperature. After a week, single crystals were obtained.

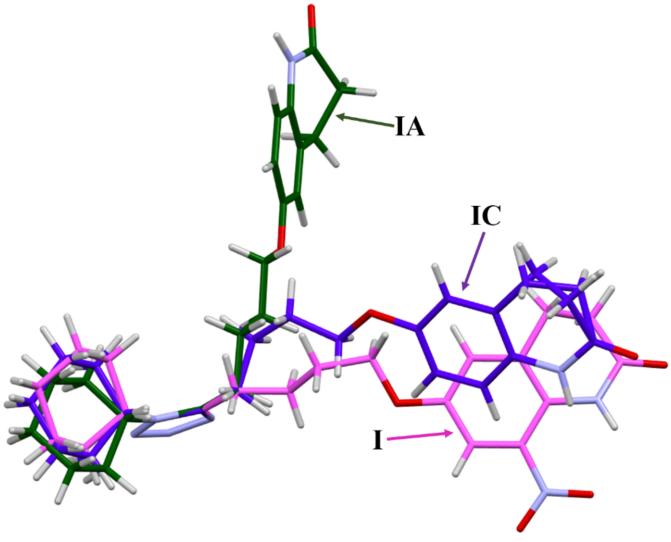

Figure 6
An overlay of structures **I**, **IA** and **IC**.

Table 3
Experimental details.

Crystal data	
Chemical formula	$C_{20}H_{26}N_6O_4$
M_r	414.47
Crystal system, space group	Triclinic, $P\overline{1}$
Temperature (K)	100
a, b, c (Å)	6.4597 (8), 9.2666 (11), 17.382 (2)
α, β, γ (°)	104.113 (5), 96.645 (5), 99.656 (5)
V (Å^3)	981.3 (2)
Z	2
Radiation type	Mo $K\alpha$
μ (mm^{-1})	0.10
Crystal size (mm)	0.24 × 0.13 × 0.05
Data collection	
Diffractometer	Bruker D8 Quest
Absorption correction	Multi-scan (*SADABS*; Krause *et al.*, 2015)
T_{min}, T_{max}	0.683, 0.746
No. of measured, independent and observed [$I > 2\sigma(I)$] reflections	16058, 5647, 4069
R_{int}	0.043
(sin $\theta/\lambda)_{max}$ (Å^{-1})	0.705
Refinement	
$R[F^2 > 2\sigma(F^2)]$, $wR(F^2)$, S	0.069, 0.141, 1.08
No. of reflections	5647
No. of parameters	275
H-atom treatment	H atoms treated by a mixture of independent and constrained refinement
$\Delta\rho_{max}$, $\Delta\rho_{min}$ (e Å^{-3})	0.36, −0.39

Computer programs: *APEX2* and *SAINT* (Bruker, 2016), *SHELXT2018/2* (Sheldrick, 2015*a*), *SHELXL2018/3* (Sheldrick, 2015*b*) and *OLEX2* (Dolomanov *et al.*, 2009).

7. Refinement

Crystal data, data collection and structure refinement details are summarized in Table 3. All of the hydrogen atoms, except H2 (attached to N2), which was located from a difference-Fourier map, were placed at their geometrically calculated positions and refined using a riding model with U_{iso}(H) = 1.2U_{eq}(C) or 1.5U_{eq}(C-methyl).

Acknowledgements

The authors are grateful to IISERB for research facilities and infrastructure. YD thanks DST-INSPIRE for the research fellowship.

References

Boeyens, J. C. A. (1978). *J. Cryst. Mol. Struct.* **8**, 317–320.
Bruker (2016). *APEX2* and *SAINT*. Bruker AXS Inc., Madison, Wisconsin, USA.
Cremer, D. & Pople, J. A. (1975). *J. Am. Chem. Soc.* **97**, 1354–1358.
Dolomanov, O. V., Bourhis, L. J., Gildea, R. J., Howard, J. A. K. & Puschmann, H. (2009). *J. Appl. Cryst.* **42**, 339–341.
Groom, C. R., Bruno, I. J., Lightfoot, M. P. & Ward, S. C. (2016). *Acta Cryst.* B**72**, 171–179.
Krause, L., Herbst-Irmer, R., Sheldrick, G. M. & Stalke, D. (2015). *J. Appl. Cryst.* **48**, 3–10.
Lauters, R. & Wilkin, D. (2002). *Am. Fam. Physician*, **105**, 4, 366–367.
Lopez-Rodriguez, R., McManus, J. A., Murphy, N. S., Ott, M. A. & Burns, M. J. (2020). *Org. Process Res. Dev.* **24**, 9, 1812–1819.
Macrae, C. F., Sovago, I., Cottrell, S. J., Galek, P. T. A., McCabe, P., Pidcock, E., Platings, M., Shields, G. P., Stevens, J. S., Towler, M. & Wood, P. A. (2020). *J. Appl. Cryst.* **53**, 226–235.
Sheldrick, G. M. (2015*a*). *Acta Cryst.* A**71**, 3–8.
Sheldrick, G. M. (2015*b*). *Acta Cryst.* C**71**, 3–8.
Spackman, M. A. & McKinnon, J. J. (2002). *CrystEngComm*, **4**, 378–392.
Spackman, P. R., Turner, M. J., McKinnon, J. J., Wolff, S. K., Grimwood, D. J., Jayatilaka, D. & Spackman, M. A. (2021). *J. Appl. Cryst.* **54**, 1006–1011.
Spek, A. L. (2020). *Acta Cryst.* E**76**, 1–11.
Vikram, H. P. R., Kumar, T. P., Kumar, G., Beeraka, N. M., Deka, R., Suhail, S. M., Jat, S., Bannimath, N., Padmanabhan, G., Chandan, R. S., Kumar, P. & Gurupadayya, B. (2024). *J. Pharm. Anal*, **14**, 5, 100919.
Whittall, L. B., Whittle, R. R. & Stowell, G. W. (2002). *Acta Cryst.* C**58**, o525–o527.
Yoshimura, M., Miyake, M., Kawato, T., Bando, M., Toda, M., Kato, Y., Fukami, T. & Ozeki, T. (2017). *Cryst. Growth Des.* **17**, 2, 550–557.

supporting information

Acta Cryst. (2025). E**81**, 284-288 [https://doi.org/10.1107/S2056989025001793]

Crystal structure and Hirshfeld surface analysis of 6-[4-(1-cyclohexyl-1*H*-tetrazol-5-yl)butoxy]-8-nitro-3,4-dihydroquinolin-2(1*H*)-one

Arnab Dutta, Yogesh Dhasmana, T. P. Mohan, B. Selvakumar and Deepak Chopra

Computing details

6-[4-(1-Cyclohexyl-1*H*-tetrazol-5-yl)butoxy]-8-nitro-3,4-dihydroquinolin-2(1*H*)-one

Crystal data

$C_{20}H_{26}N_6O_4$
$M_r = 414.47$
Triclinic, $P\overline{1}$
$a = 6.4597$ (8) Å
$b = 9.2666$ (11) Å
$c = 17.382$ (2) Å
$\alpha = 104.113$ (5)°
$\beta = 96.645$ (5)°
$\gamma = 99.656$ (5)°
$V = 981.3$ (2) Å^3
$Z = 2$
$F(000) = 440$
$D_x = 1.403$ Mg m^{-3}
Mo $K\alpha$ radiation, $\lambda = 0.71073$ Å
Cell parameters from 4187 reflections
$\theta = 2.5$–30.0°
$\mu = 0.10$ mm^{-1}
$T = 100$ K
Plate, yellow
0.24 × 0.13 × 0.05 mm

Data collection

Bruker D8 Quest diffractometer
Radiation source: microfocus sealed X-ray tube, Incoatec Iμs
Mirror optics monochromator
Detector resolution: 7.9 pixels mm^{-1}
ω and φ scans
Absorption correction: multi-scan (SADABS; Krause *et al.*, 2015)
$T_{min} = 0.683$, $T_{max} = 0.746$
16058 measured reflections
5647 independent reflections
4069 reflections with $I > 2\sigma(I)$
$R_{int} = 0.043$
$\theta_{max} = 30.1°$, $\theta_{min} = 2.3°$
$h = -9\rightarrow9$
$k = -12\rightarrow13$
$l = -24\rightarrow24$

Refinement

Refinement on F^2
Least-squares matrix: full
$R[F^2 > 2\sigma(F^2)] = 0.069$
$wR(F^2) = 0.141$
$S = 1.08$
5647 reflections
275 parameters
0 restraints
Primary atom site location: structure-invariant direct methods
Hydrogen site location: mixed
H atoms treated by a mixture of independent and constrained refinement
$w = 1/[\sigma^2(F_o^2) + (0.036P)^2 + 1.0039P]$ where $P = (F_o^2 + 2F_c^2)/3$
$(\Delta/\sigma)_{max} < 0.001$
$\Delta\rho_{max} = 0.36$ e Å^{-3}
$\Delta\rho_{min} = -0.39$ e Å^{-3}

Special details

Geometry. All esds (except the esd in the dihedral angle between two l.s. planes) are estimated using the full covariance matrix. The cell esds are taken into account individually in the estimation of esds in distances, angles and torsion angles; correlations between esds in cell parameters are only used when they are defined by crystal symmetry. An approximate (isotropic) treatment of cell esds is used for estimating esds involving l.s. planes.

Fractional atomic coordinates and isotropic or equivalent isotropic displacement parameters (Å²)

	x	*y*	*z*	U_{iso}*/U_{eq}
O4	0.3538 (2)	0.31868 (16)	0.63879 (8)	0.0143 (3)
O3	0.2010 (2)	−0.53087 (16)	0.43484 (9)	0.0182 (3)
O1	0.1523 (3)	−0.15696 (17)	0.33108 (8)	0.0196 (3)
O2	0.2294 (2)	0.08708 (17)	0.35239 (9)	0.0189 (3)
N1	0.2034 (3)	−0.0266 (2)	0.37737 (10)	0.0127 (3)
N2	0.1868 (3)	−0.28422 (19)	0.45172 (10)	0.0120 (3)
N3	1.0704 (3)	0.8204 (2)	0.79866 (10)	0.0163 (4)
N4	0.9390 (3)	1.01503 (19)	0.85030 (10)	0.0132 (3)
N15	1.2241 (3)	0.9502 (2)	0.81932 (11)	0.0195 (4)
N16	1.1471 (3)	1.0679 (2)	0.85096 (11)	0.0184 (4)
C4	0.3116 (3)	0.1701 (2)	0.59483 (11)	0.0113 (4)
C6	0.2611 (3)	−0.1011 (2)	0.58111 (11)	0.0107 (4)
C3	0.2731 (3)	0.1415 (2)	0.51206 (11)	0.0115 (4)
H3	0.272801	0.223263	0.488058	0.014*
C1	0.2277 (3)	−0.1325 (2)	0.49707 (11)	0.0108 (4)
C5	0.3044 (3)	0.0472 (2)	0.62909 (11)	0.0114 (4)
H5	0.329520	0.066015	0.685933	0.014*
C2	0.2347 (3)	−0.0072 (2)	0.46401 (11)	0.0109 (4)
C14	0.8946 (3)	0.8632 (2)	0.81830 (11)	0.0132 (4)
C9	0.2296 (3)	−0.4038 (2)	0.48070 (12)	0.0130 (4)
C17	0.7998 (3)	1.1125 (2)	0.88721 (12)	0.0137 (4)
H17	0.650785	1.068434	0.858439	0.016*
C10	0.3854 (3)	0.3463 (2)	0.72468 (11)	0.0147 (4)
H10A	0.507798	0.304216	0.742582	0.018*
H10B	0.257221	0.295982	0.741387	0.018*
C7	0.2393 (3)	−0.2331 (2)	0.61839 (12)	0.0129 (4)
H7A	0.088266	−0.265566	0.622944	0.015*
H7B	0.323372	−0.199896	0.673263	0.015*
C13	0.6805 (3)	0.7660 (2)	0.81081 (13)	0.0178 (4)
H13A	0.572194	0.814652	0.787945	0.021*
H13B	0.653491	0.763306	0.865403	0.021*
C11	0.4277 (3)	0.5164 (2)	0.76270 (12)	0.0150 (4)
H11A	0.408954	0.534190	0.819755	0.018*
H11B	0.319495	0.559413	0.735488	0.018*
C8	0.3162 (3)	−0.3673 (2)	0.56840 (12)	0.0145 (4)
H8A	0.473662	−0.343760	0.575942	0.017*
H8B	0.272399	−0.457746	0.588016	0.017*
C18	0.8604 (4)	1.2733 (2)	0.87864 (13)	0.0184 (4)
H18A	0.849021	1.270559	0.820994	0.022*

H18B	1.009626	1.318310	0.904730	0.022*
C12	0.6491 (3)	0.6027 (2)	0.75913 (12)	0.0156 (4)
H12A	0.759748	0.552795	0.779382	0.019*
H12B	0.661840	0.602030	0.702839	0.019*
C22	0.8051 (4)	1.1126 (2)	0.97530 (13)	0.0178 (4)
H22A	0.762243	1.007088	0.978963	0.021*
H22B	0.951825	1.153979	1.004952	0.021*
C21	0.6549 (4)	1.2086 (3)	1.01333 (13)	0.0198 (5)
H21A	0.663914	1.210730	1.070855	0.024*
H21B	0.506652	1.162545	0.986406	0.024*
C20	0.7128 (4)	1.3703 (3)	1.00564 (13)	0.0204 (5)
H20A	0.609442	1.429620	1.028136	0.024*
H20B	0.855917	1.419567	1.036988	0.024*
C19	0.7118 (4)	1.3706 (3)	0.91805 (13)	0.0212 (5)
H19A	0.756991	1.476331	0.915033	0.025*
H19B	0.565143	1.331179	0.888035	0.025*
H2	0.150 (3)	−0.304 (2)	0.3988 (13)	0.009 (5)*

Atomic displacement parameters (Å²)

	U^{11}	U^{22}	U^{33}	U^{12}	U^{13}	U^{23}
O4	0.0222 (8)	0.0082 (7)	0.0122 (7)	0.0025 (6)	0.0026 (6)	0.0022 (5)
O3	0.0195 (8)	0.0090 (7)	0.0240 (8)	0.0019 (6)	0.0062 (6)	0.0001 (6)
O1	0.0264 (9)	0.0162 (8)	0.0129 (7)	0.0035 (7)	0.0015 (6)	−0.0008 (6)
O2	0.0257 (9)	0.0179 (8)	0.0157 (7)	0.0047 (7)	0.0037 (6)	0.0092 (6)
N1	0.0091 (8)	0.0150 (8)	0.0137 (8)	0.0029 (7)	0.0016 (6)	0.0031 (6)
N2	0.0133 (8)	0.0093 (8)	0.0116 (8)	0.0009 (6)	0.0013 (6)	0.0009 (6)
N3	0.0156 (9)	0.0174 (9)	0.0159 (8)	0.0055 (7)	0.0039 (7)	0.0023 (7)
N4	0.0120 (8)	0.0123 (8)	0.0151 (8)	0.0027 (7)	0.0035 (6)	0.0024 (6)
N15	0.0168 (9)	0.0205 (10)	0.0203 (9)	0.0049 (8)	0.0061 (7)	0.0019 (7)
N16	0.0123 (9)	0.0189 (9)	0.0225 (9)	0.0002 (7)	0.0046 (7)	0.0039 (7)
C4	0.0090 (9)	0.0095 (9)	0.0160 (9)	0.0032 (7)	0.0033 (7)	0.0032 (7)
C6	0.0088 (9)	0.0110 (9)	0.0143 (9)	0.0035 (7)	0.0045 (7)	0.0049 (7)
C3	0.0095 (9)	0.0110 (9)	0.0156 (9)	0.0020 (7)	0.0033 (7)	0.0059 (7)
C1	0.0077 (9)	0.0100 (9)	0.0151 (9)	0.0015 (7)	0.0038 (7)	0.0033 (7)
C5	0.0108 (9)	0.0128 (9)	0.0106 (8)	0.0013 (8)	0.0025 (7)	0.0033 (7)
C2	0.0075 (9)	0.0139 (10)	0.0112 (9)	0.0014 (7)	0.0014 (7)	0.0035 (7)
C14	0.0168 (10)	0.0118 (9)	0.0100 (8)	0.0037 (8)	0.0013 (7)	0.0010 (7)
C9	0.0093 (9)	0.0093 (9)	0.0215 (10)	0.0020 (7)	0.0066 (8)	0.0046 (8)
C17	0.0120 (10)	0.0110 (9)	0.0172 (9)	0.0035 (8)	0.0031 (8)	0.0009 (7)
C10	0.0205 (11)	0.0117 (10)	0.0111 (9)	0.0021 (8)	0.0025 (8)	0.0026 (7)
C7	0.0165 (10)	0.0083 (9)	0.0141 (9)	0.0012 (8)	0.0030 (8)	0.0042 (7)
C13	0.0150 (11)	0.0139 (10)	0.0213 (10)	0.0015 (8)	0.0043 (8)	−0.0008 (8)
C11	0.0197 (11)	0.0116 (10)	0.0131 (9)	0.0034 (8)	0.0041 (8)	0.0014 (7)
C8	0.0157 (10)	0.0108 (9)	0.0186 (10)	0.0025 (8)	0.0040 (8)	0.0064 (8)
C18	0.0255 (12)	0.0153 (10)	0.0179 (10)	0.0070 (9)	0.0080 (9)	0.0066 (8)
C12	0.0185 (11)	0.0104 (9)	0.0174 (10)	0.0043 (8)	0.0041 (8)	0.0016 (8)
C22	0.0225 (11)	0.0137 (10)	0.0216 (10)	0.0065 (9)	0.0092 (9)	0.0083 (8)

C21	0.0213 (12)	0.0216 (11)	0.0209 (11)	0.0097 (9)	0.0086 (9)	0.0077 (9)
C20	0.0277 (12)	0.0163 (11)	0.0186 (10)	0.0118 (9)	0.0045 (9)	0.0021 (8)
C19	0.0309 (13)	0.0162 (11)	0.0203 (10)	0.0096 (10)	0.0065 (9)	0.0078 (9)

Geometric parameters (Å, º)

O4—C4	1.366 (2)	C10—H10B	0.9900
O4—C10	1.436 (2)	C10—C11	1.517 (3)
O3—C9	1.221 (2)	C7—H7A	0.9900
O1—N1	1.243 (2)	C7—H7B	0.9900
O2—N1	1.228 (2)	C7—C8	1.526 (3)
N1—C2	1.458 (2)	C13—H13A	0.9900
N2—C1	1.398 (2)	C13—H13B	0.9900
N2—C9	1.379 (2)	C13—C12	1.526 (3)
N2—H2	0.89 (2)	C11—H11A	0.9900
N3—N15	1.367 (3)	C11—H11B	0.9900
N3—C14	1.319 (3)	C11—C12	1.533 (3)
N4—N16	1.349 (2)	C8—H8A	0.9900
N4—C14	1.348 (3)	C8—H8B	0.9900
N4—C17	1.470 (3)	C18—H18A	0.9900
N15—N16	1.301 (3)	C18—H18B	0.9900
C4—C3	1.383 (3)	C18—C19	1.531 (3)
C4—C5	1.404 (3)	C12—H12A	0.9900
C6—C1	1.401 (3)	C12—H12B	0.9900
C6—C5	1.386 (3)	C22—H22A	0.9900
C6—C7	1.511 (3)	C22—H22B	0.9900
C3—H3	0.9500	C22—C21	1.523 (3)
C3—C2	1.391 (3)	C21—H21A	0.9900
C1—C2	1.412 (3)	C21—H21B	0.9900
C5—H5	0.9500	C21—C20	1.525 (3)
C14—C13	1.491 (3)	C20—H20A	0.9900
C9—C8	1.496 (3)	C20—H20B	0.9900
C17—H17	1.0000	C20—C19	1.522 (3)
C17—C18	1.524 (3)	C19—H19A	0.9900
C17—C22	1.527 (3)	C19—H19B	0.9900
C10—H10A	0.9900		

C4—O4—C10	116.53 (15)	C14—C13—H13A	108.4
O1—N1—C2	119.39 (16)	C14—C13—H13B	108.4
O2—N1—O1	121.98 (17)	C14—C13—C12	115.69 (18)
O2—N1—C2	118.62 (17)	H13A—C13—H13B	107.4
C1—N2—H2	117.8 (14)	C12—C13—H13A	108.4
C9—N2—C1	124.94 (17)	C12—C13—H13B	108.4
C9—N2—H2	116.4 (14)	C10—C11—H11A	108.5
C14—N3—N15	105.82 (17)	C10—C11—H11B	108.5
N16—N4—C17	122.55 (17)	C10—C11—C12	114.99 (17)
C14—N4—N16	108.70 (17)	H11A—C11—H11B	107.5
C14—N4—C17	128.46 (18)	C12—C11—H11A	108.5

N16—N15—N3	110.93 (17)	C12—C11—H11B	108.5
N15—N16—N4	106.10 (17)	C9—C8—C7	112.55 (17)
O4—C4—C3	117.16 (17)	C9—C8—H8A	109.1
O4—C4—C5	123.72 (17)	C9—C8—H8B	109.1
C3—C4—C5	119.11 (18)	C7—C8—H8A	109.1
C1—C6—C7	118.46 (17)	C7—C8—H8B	109.1
C5—C6—C1	120.91 (18)	H8A—C8—H8B	107.8
C5—C6—C7	120.58 (17)	C17—C18—H18A	109.8
C4—C3—H3	120.1	C17—C18—H18B	109.8
C4—C3—C2	119.86 (18)	C17—C18—C19	109.59 (18)
C2—C3—H3	120.1	H18A—C18—H18B	108.2
N2—C1—C6	118.42 (17)	C19—C18—H18A	109.8
N2—C1—C2	124.44 (17)	C19—C18—H18B	109.8
C6—C1—C2	117.13 (18)	C13—C12—C11	108.81 (17)
C4—C5—H5	119.5	C13—C12—H12A	109.9
C6—C5—C4	120.92 (18)	C13—C12—H12B	109.9
C6—C5—H5	119.5	C11—C12—H12A	109.9
C3—C2—N1	116.24 (17)	C11—C12—H12B	109.9
C3—C2—C1	122.02 (17)	H12A—C12—H12B	108.3
C1—C2—N1	121.74 (17)	C17—C22—H22A	109.6
N3—C14—N4	108.44 (18)	C17—C22—H22B	109.6
N3—C14—C13	128.13 (19)	H22A—C22—H22B	108.1
N4—C14—C13	123.40 (18)	C21—C22—C17	110.43 (18)
O3—C9—N2	119.85 (19)	C21—C22—H22A	109.6
O3—C9—C8	123.46 (19)	C21—C22—H22B	109.6
N2—C9—C8	116.67 (17)	C22—C21—H21A	109.5
N4—C17—H17	108.0	C22—C21—H21B	109.5
N4—C17—C18	111.43 (17)	C22—C21—C20	110.50 (18)
N4—C17—C22	109.98 (17)	H21A—C21—H21B	108.1
C18—C17—H17	108.0	C20—C21—H21A	109.5
C18—C17—C22	111.33 (17)	C20—C21—H21B	109.5
C22—C17—H17	108.0	C21—C20—H20A	109.5
O4—C10—H10A	109.9	C21—C20—H20B	109.5
O4—C10—H10B	109.9	H20A—C20—H20B	108.0
O4—C10—C11	108.84 (16)	C19—C20—C21	110.93 (18)
H10A—C10—H10B	108.3	C19—C20—H20A	109.5
C11—C10—H10A	109.9	C19—C20—H20B	109.5
C11—C10—H10B	109.9	C18—C19—H19A	109.3
C6—C7—H7A	109.3	C18—C19—H19B	109.3
C6—C7—H7B	109.3	C20—C19—C18	111.82 (18)
C6—C7—C8	111.54 (16)	C20—C19—H19A	109.3
H7A—C7—H7B	108.0	C20—C19—H19B	109.3
C8—C7—H7A	109.3	H19A—C19—H19B	107.9
C8—C7—H7B	109.3		

O4—C4—C3—C2	178.34 (18)	C1—N2—C9—C8	3.3 (3)
O4—C4—C5—C6	−179.89 (18)	C1—C6—C5—C4	1.3 (3)
O4—C10—C11—C12	−74.1 (2)	C1—C6—C7—C8	34.9 (2)

O3—C9—C8—C7	−151.93 (19)	C5—C4—C3—C2	−2.1 (3)
O1—N1—C2—C3	−174.48 (18)	C5—C6—C1—N2	179.37 (18)
O1—N1—C2—C1	6.0 (3)	C5—C6—C1—C2	−1.6 (3)
O2—N1—C2—C3	5.7 (3)	C5—C6—C7—C8	−147.74 (19)
O2—N1—C2—C1	−173.81 (18)	C14—N3—N15—N16	0.5 (2)
N2—C1—C2—N1	−1.5 (3)	C14—N4—N16—N15	0.6 (2)
N2—C1—C2—C3	179.02 (19)	C14—N4—C17—C18	−152.15 (19)
N2—C9—C8—C7	29.8 (2)	C14—N4—C17—C22	83.9 (2)
N3—N15—N16—N4	−0.7 (2)	C14—C13—C12—C11	176.09 (17)
N3—C14—C13—C12	−13.5 (3)	C9—N2—C1—C6	−17.8 (3)
N4—C14—C13—C12	168.87 (18)	C9—N2—C1—C2	163.28 (19)
N4—C17—C18—C19	−179.86 (17)	C17—N4—N16—N15	175.00 (17)
N4—C17—C22—C21	−177.90 (18)	C17—N4—C14—N3	−174.26 (18)
N15—N3—C14—N4	−0.1 (2)	C17—N4—C14—C13	3.8 (3)
N15—N3—C14—C13	−178.08 (19)	C17—C18—C19—C20	55.8 (3)
N16—N4—C14—N3	−0.3 (2)	C17—C22—C21—C20	−57.1 (2)
N16—N4—C14—C13	177.78 (18)	C10—O4—C4—C3	177.68 (17)
N16—N4—C17—C18	34.6 (3)	C10—O4—C4—C5	−1.9 (3)
N16—N4—C17—C22	−89.3 (2)	C10—C11—C12—C13	−171.11 (17)
C4—O4—C10—C11	−179.44 (17)	C7—C6—C1—N2	−3.3 (3)
C4—C3—C2—N1	−177.77 (17)	C7—C6—C1—C2	175.74 (17)
C4—C3—C2—C1	1.8 (3)	C7—C6—C5—C4	−175.97 (18)
C6—C1—C2—N1	179.61 (18)	C18—C17—C22—C21	58.1 (2)
C6—C1—C2—C3	0.1 (3)	C22—C17—C18—C19	−56.7 (2)
C6—C7—C8—C9	−47.1 (2)	C22—C21—C20—C19	56.3 (3)
C3—C4—C5—C6	0.5 (3)	C21—C20—C19—C18	−56.1 (3)
C1—N2—C9—O3	−175.10 (18)		